Durability Assessment of Expansive and Nonexpansive Calcium Sulfoaluminate Belite Cement Concrete in Chloride-Rich Environments

Paul Shaji[1] and Piyush Chaunsali, Ph.D., A.M.ASCE[2]

Abstract: Calcium sulfoaluminate belite (CSAB) cement has gained prominence as a viable environmentally friendly substitute for conventional portland cement (PC). The current study investigates the relative performance of expansive and nonexpansive CSAB cement-based concretes, and PC-based concretes when subjected to chloride-rich conditions. Multiple testing methodologies, including surface resistivity measurements, chloride migration, rapid chloride penetration, long-term bulk diffusion, and water sorptivity, were employed to assess the durability of these concrete systems. Surface resistivity measurements indicated that CSAB systems exhibited significantly higher resistivity when compared with PC-based counterparts. Increased resistivity in CSAB systems was influenced by the conductivity of the pore solution, emphasizing that the formation factor provides a more accurate representation of the pore structure within the system. The expansive and nonexpansive CSAB cement–based concrete outperformed PC-based concrete in migration-based tests and rapid chloride penetration test (RCPT). In contrast, the CSAB and PC systems demonstrated similar performance in the long-term bulk diffusion-based test. Although CSAB systems exhibit finer pore structures than PC-based counterparts, their performance in chloride-rich environments is affected by their reduced binding capacity. The study emphasizes that the conclusions drawn from accelerated tests and resistivity measurements of CSAB cement–based concrete must be cautiously interpreted because these results may not indicate real-world performance. **DOI: 10.1061/JMCEE7.MTENG-17544.**

Author keywords: Calcium sulfoaluminate belite (CSAB) cement; Chloride transport; Expansive cement; Ettringite; Gypsum.

Introduction

Calcium sulfoaluminate belite (CSAB) cement is an environmentally friendly alternative to portland cement (PC) (Chaunsali and Vaishnav 2020; Gartner 2004; Juenger et al. 2011). The CO_2 emissions during CSAB cement manufacturing have been reported to be lower than the CO_2 emissions during PC production (Hanein et al. 2018; Zhou et al. 2006). Ye'elimite ($C_4A_3\$$) is the main component of CSAB cement, along with belite (C_2S), calcium aluminoferrite (C_4AF), and calcium sulfate ($C\$$) (Glasser and Zhang 2001). The phase assemblage formed during the hydration of CSAB cementitious system is significantly different from that of PC. The major hydration products formed consist of ettringite, monosulfate, and the noncrystalline form of aluminum hydroxide. The amount of sulfate in a CSAB-based cementitious system is an important parameter that influences the hydrated phase assemblage because monosulfate formation will only occur in the absence or meagre availability of calcium sulfate. The amount of calcium sulfate in the system can be regulated to control the expansive behavior of the CSAB cement system. However, such system will be devoid of monosulfate as the presence of gypsum is on the higher side (i.e., molar ratio: $C\$/C_4A_3\$ > 2$) (Bizzozero et al. 2014; Chen et al. 2012; Hargis et al. 2018).

The chloride transport through the cover concrete depends on the cementitious system's tortuosity and binding capability. The binding capacity of hydrated PC is dependent on the ion-exchange characteristics of themonosulfate (AFm) phase and physical adsorption by calcium silicate hydrate (C—S—H) (Florea and Brouwers 2012). Similar to PC, the capacity of CSAB cement system in binding chlorides is mainly attributed to the presence of AFm (Jen et al. 2017; Paul et al. 2015). The presence of gypsum facilitates the formation of ettringite (AFt) and inhibits AFm generation due to the supply of SO_4^{2-} ions. The absence of AFm in hydrated CSAB cement will reduce its chemical binding capacity (Jiang et al. 2019).

Besides binding, an alternative approach to minimize chloride ingress is to decrease the pore interconnectivity of the cementitious system. The literature on the resistance of CSAB system against chloride ingress is limited and contradicting. Zhao et al. (2014) reported that the CSAB system had a better resistance against chloride ion permeability when compared with PC, even when these systems were exposed to freeze–thaw cycles. Similar observations were also noted by Ioannou et al. (2015), where a blend of a calcium sulfoaluminate (CSA) system with fly ash was observed to perform better than PC). The improved performance of the CSAB system was attributed to a well-refined pore structure of these systems. The performance of these systems in a chloride environment was assessed with the help of accelerated migration-based test methods. The accelerated test results may be highly influenced by the pore solution conductivity and pore refinement of the system. Furthermore, clarity on the role of chloride binding in these systems and its influence on the chloride resistance is lacking, and thereby should be assessed using long-term bulk diffusion-based tests.

[1]Ph.D. Research Scholar, Dept. of Civil Engineering, Indian Institute of Technology Madras, Chennai 600036, India. Email: paulshaji123@gmail.com

[2]Assistant Professor, Dept. of Civil Engineering, Indian Institute of Technology Madras, Chennai 600036, India (corresponding author). ORCID: https://orcid.org/0000-0003-2107-6488. Email: pchaunsali@iitm.ac.in

Note. This manuscript was submitted on August 21, 2023; approved on January 12, 2024; published online on May 2, 2024. Discussion period open until October 2, 2024; separate discussions must be submitted for individual papers. This paper is part of the ***Journal of Materials in Civil Engineering***, © ASCE, ISSN 0899-1561.

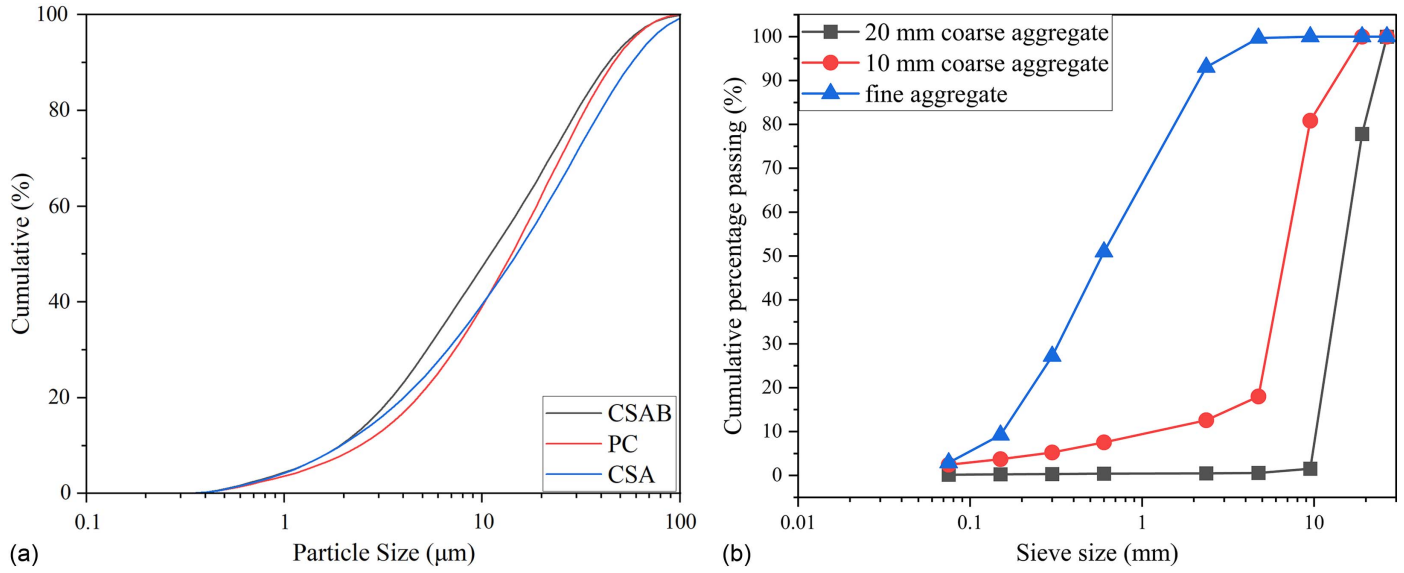

Fig. 1. Particle size distribution of (a) binders; and (b) aggregates.

However, Alapati et al. (2022) showed that the CSA cement system having high belite content had less chloride binding capacity, resulting in a higher ingress of chloride ions when compared with PC. The high-belite CSA system was observed to have a much coarser pore structure than PC, which contradicts the observations made by Ioannou et al. (2015) and Zhao et al. (2014). The reduced pore refinement may be attributed to the difference in the CSA cement composition used for these studies. Nevertheless, the influence of chloride binding on CSAB systems having higher ye'elimite content needs further clarification.

Also, the effect of gypsum addition on the chloride resistance and the binding capability of CSAB system lacks clarity. Although the presence of gypsum reduces the binding capability of the system, it improves the tortuosity. Hence, a comprehensive study is required to understand the synergetic effect of binding and pore refinement on the resistance of the CSAB cementitious system against chloride ingress.

The expansive CSAB cement concrete produced by adding gypsum to ye'elimite-rich CSAB cement is an ettringite-rich system. The calcium sulfate to ye'elimite molar ratio of the expansive system under consideration in this study is around 2.66. Although different studies have examined the effect of admixing gypsum on the chloride resistance of CSAB cement, such studies were limited to a calcium sulfate to ye'elimite molar ratio of less than 2. The increase in the calcium sulfate to ye'elimite molar ratio of a CSAB system having high ye'elimite content can produce more ettringite and can cause expansion. Furthermore, the additional ettringite formed may influence the pore structure of the system.

However, such a system will lack monosulfate and will be lacking in its capability to bind chlorides. Although such systems will be devoid of monosulfate, the additional ettringite formation, if controlled, will result in pore refinement. The pore densification due to ettringite formation in such expansive CSAB can be critical in influencing the chloride resistance of the system. Studies that assessed the chloride resistance of such ettringite-rich systems are limited. The current study examines an ettringite-rich expansive CSAB system and a nonexpansive CSAB system to understand their resistance against chloride ingress. The study also examines the performance of CSAB-based concretes against PC-based concrete having similar strength levels.

Materials

The raw materials used in this research consisted of PC of 53 grade conforming to IS 269 (BIS 2015), commercially available CSAB cement of 42.5 grade, calcium sulfoaluminate admixture, and laboratory-grade gypsum (calcium sulfate dihydrate). The particle size distributions of PC, CSA admixture, and CSAB cement are shown in Fig. 1. The CSAB cement exhibited a lower particle size distribution in comparison with PC. The d_{50} particle size measurements for CSAB cement, CSA admixture, and PC were recorded as 12.6, 17, and 16 μm, respectively. The specific gravity values of CSAB cement and CSA admixture were found to be 2.84 and 3.07, comparatively lower than that of PC cement.

Oxide and phase compositions of raw materials, as given in Tables 1 and 2, were determined by X-ray fluorescence (XRF) and quantitative X-ray diffraction (QXRD), respectively. The commercially procured CSAB and PC cement systems were not expansive in nature. However, PC and CSAB systems can be converted into expansive systems with the addition of 10% CSA admixture and 15% gypsum, respectively (Shenbagam et al. 2021; Shenbagam and Chaunsali 2022).

Table 1. Oxide composition (% by weight) of raw materials obtained by XRF

Oxide	PC	CSA[a]	CSAB[b]
CaO	61.3	62.0	38.8
SiO_2	21.1	2.6	13.1
Al_2O_3	6.3	2.5	22.6
SO_3	3.3	28.4	16.7
Fe_2O_3	5.1	1.5	3.4
MgO	1.1	2.2	2.9
Na_2O	0.0	0.0	0.1
K_2O	0.8	0.3	0.6
TiO_2	0.6	0	0.9
SrO	0.0	0.2	0.2

[a]Used as an admixture with PC.
[b]Used as a sole binder.

J. Mater. Civ. Eng., 2024, 36(7): 04024195

Table 2. Phase composition (% by weight) of binders

Phases	PC	CSA	CSAB
Alite	48.0	0	0
Belite	25.9	10.3	22.3
Tricalcium aluminate	8.4	0	2.2
Tetracalcium aluminoferrite	6.5	1.2	0
Ye'elimite	0	14.5	48.8
Anhydrite	0	44.7	19.3
Lime	0	21.9	0
Gypsum	3.2	0	1.4
Dolomite	0	5.7	3.4
Calcite	4.7	0	0

Experimental Methods

Mixture Proportioning

Cement paste samples were prepared at a water-to-binder ratio (w/b) of 0.5 (by mass) as specified in ASTM C305 (ASTM 2020). All materials were conditioned for 24 h before casting. The paste samples were used for microstructural characterization. The materials were initially mixed with a front-mounted planetary Hobart mixer in a controlled environment of 25°C ± 2°C. The initial mixing was performed in a dry state to ensure uniform and homogeneous mixing. Prismatic specimens of dimensions 25 × 25 × 285 mm were cast and immediately sealed in thin polyethene cling wraps to prevent water loss due to evaporation and kept in the aforementioned controlled environment for 24 h. The prismatic specimens were demolded after 24 h and cured in a mist room [relative humidity (RH) greater than 90%] for 28 days to avoid leaching of any hydration products. Concrete mixtures of M30 grade [as per Indian Standard 456 (BIS 2000)] were designed.

To achieve a characteristic compressive strength of 30 MPa, an average compressive strength (of 100 × 100 × 100-mm specimens) in the range of 38–43 MPa was considered. River sand conforming to Zone 2 according to IS:383 (BIS 2016) was used as fine aggregate along with granite-based coarse aggregate consisting of 10- and 20-mm aggregates. The 10- and 20-mm aggregates were mixed in a ratio of 40:60, respectively (IS:383). The gradation of aggregates used is provided in Fig. 1. The mix was optimized to achieve a target slump of 70–120 mm with the help of PCE-based superplasticizers (SP) with solid content of 34%. The details of the concrete mixtures under consideration are provided in Tables 3 and 4. A pan mixer was used for mixing concrete at 25 revolutions/min (rpm). Subsequently, the specimens were cast into various molds and placed in normal atmospheric conditions for 24 h, followed by 28 days of curing in a mist room (RH > 90%).

Table 3. Mix proportions (% by weight) of binders used in the study

Nomenclature	PC	CSA admixture	CSAB cement	Gypsum	Characteristics
PC	100	0	—	—	Nonexpansive
PC_CSA	90	10	—	—	Expansive
CSAB	—	—	100	0	Nonexpansive
CSAB_E_G	—	—	85	15	Expansive

Microstructural Characterization

Microstructural characterization was performed using paste samples prepared as mentioned in the section "Mixture Proportioning." The prisms of size 25 × 25 × 285 mm were cut into thin slices of about 3–5-mm thickness using a diamond saw. The hydration stoppage was performed using the solvent exchange method. The paste samples were immersed in isopropyl alcohol (IPA) for 3 days, and IPA was replenished after the first day. The samples removed from IPA were stored in a vacuum desiccator in the presence of silica gel for at least 3 days before being used for characterization studies (Dhandapani and Santhanam 2017). The paste samples remained in the vacuum desiccator till the date of testing.

The paste samples were ground to a powder and passed through a 75-μm sieve for conducting X-ray diffraction (XRD) and thermogravimetric analysis (TGA). Mercury intrusion porosimetry (MIP) was performed utilizing small chunks of paste sample weighing about 1 g broken off from the thin slices of paste. Furthermore, pore solution was extracted from the paste specimens prepared as per the section "Mixture Proportioning" to determine the formation factor. The pore solution conductivity was determined using an Oakton PC 2700 conductivity meter (Cole-Parmer, Vernon Hills, Illinois).

X-Ray Diffraction

The XRD equipment used for the study was a MiniFlex Rigaku (Japan) benchtop powder X-ray diffraction equipment. CuKα radiation (wavelength of 1.5405 Å) produced at 45 kV and 15 mA was used. The XRD scan was performed in the two-theta (2θ) range of 5°–70° with a step size of 0.01° and a scan rate of 10°/min. The XRD data were analyzed using X'Pert HighScore Plus software (version 3.0) along with Rietveld refinement.

Thermogravimetric Analysis

TGA was performed with SDT 650 simultaneous thermal analyzer equipment (TA Instruments, New Castle, Delaware). The test was conducted at a temperature range varying from 30°C to 900°C at a heating rate of 15°C per minute. The sample of ~15 mg was tested in a nitrogen-purged environment utilizing crucibles made from alumina.

Mercury Intrusion Porosimetry

Mercury intrusion porosimetry was performed using Thermo Scientific Pascal 140–440 equipment (Waltham, Massachusetts). The MIP equipment used for the testing is a combination of two instruments. The first instrument applied pressure ranging from 0 to 400 kPa, and the second instrument exerted pressure within the range of 0.1 to 300 MPa. The extensive range of pressure utilized in this study enables the apparatus to assess the size of pores, ranging

Table 4. Mix design of concretes used in the study

Grade	Notation	w/b	PC (kg/m^3)	CSAB (kg/m^3)	CSA (kg/m^3)	Gypsum (kg/m^3)	Water (kg/m^3)	Fine aggregate (kg/m^3)	Coarse aggregate (kg/m^3)	SP dosage (% by weight of binder)
M30	CSAB	0.5	—	360	—	—	180	743	1,115	0.4
	CSAB_E_G	0.5	—	306	—	54	180	739	1,108	0.4
	PC	0.5	360	—	—	—	180	757	1,135	0.3
	PC_CSA	0.5	324	—	36	—	180	756	1,134	0.3

from 200 μm to approximately 5 nm. The samples that had their water replaced, as mentioned in the section "Microstructural Characterization," were used for the test.

The conditioned samples were split into small pieces consisting of four to five numbers measuring approximately 5 mm in size and were utilized for testing. The rates of pressure increment for the first and the second instrument were 6 kPa/s and 6 MPa/s, respectively, along with a contact angle of 140° and surface tension of 0.48 N/m.

Characterization of Microstructural Changes due to Ingress of Chlorides

The paste specimens prepared as per the preceding sections were cut into different thin slices of 4–5 mm in size (using a diamond saw) after curing for 28 days in the mist room. The paste samples of different cementitious systems were immersed in a 3M concentrated chloride solution for 35 days. After chloride immersion, the sample was submerged in IPA for 3 days, with IPA being replenished after the first day to remove the moisture content. The samples were then stored in a vacuum desiccator until characterization tests. XRD and TGA were used to monitor the changes in microstructure of CSAB cementitious systems due to chloride ingress.

Testing Methodology

Compressive Strength

Compressive strength test was conducted on 100-mm cubes. The test was conducted as per IS 516 (BIS 2018) for different concrete systems after 3, 7, and 28 days of curing in the mist room. The equipment used for compression testing had a capacity of 3,000 kN with an accuracy of ±1%.

Water Sorptivity and Total Porosity of Concrete

Water sorptivity test was conducted as per the South African *Durability Index Testing Procedure Manual* (Alexander et al. 2018). The specimens were prepared from concrete cubes (size: 150 × 150 × 150 mm) after 28 days of curing. Cylindrical cores of diameter equal to 70 mm were obtained from concrete cubes using a diamond-tipped core cutter. Four concrete specimens of 70-mm diameter and 30-mm thickness were obtained from the cores. The specimens were then kept in an oven at 50°C for 7 days, after which they were allowed to cool down to a temperature of 23°C ± 2°C.

After measuring the initial mass, the specimens were tested for water sorptivity by placing them in a container in such a way that saturated lime solution would fill up the container to a limit of about 2 mm from the bottom side of the specimen. Also, specimens' mass readings were taken at various time intervals, as per the recommendations provided in the *Durability Index Testing Procedure Manual* (Alexander et al. 2018). The final mass was measured postvacuum saturation and 18 ± 1 h of soaking to calculate the porosity of the specimen. The water sorptivity and porosity values were calculated as an average of four specimens.

Resistivity of Concrete

Surface resistivity of various cementitious systems was evaluated using a Wenner 4 probe resistivity meter manufactured by Proceq (Schwerzenbach, Switzerland). The resistivity was measured on cylindrical specimens of dimensions 100-mm diameter and 200-mm height. The surface resistivity measurements for all the cementitious systems were taken after 3, 7, and 28 days of curing in the mist room. Three readings were taken from three locations in a single cylinder, and resistivity measurements were taken on three cylinders. Furthermore, to avoid the effect of specimen drying on the concrete samples, the resistivity measurement was taken immediately after the specimens were taken out from the mist room.

Rapid Chloride Penetration Test

The rapid chloride penetration test (RCPT) test was conducted as per ASTM C1202 (ASTM 2019). Three concrete cylinders of approximately 50-mm thickness and 100-mm diameter were made from a cylinder having a 100-mm diameter and 200-mm height after 28 days of curing. The standard test duration consisted of 6 h, and a potential of 60 V was applied to saturated specimens throughout the test period. The total charge passed was estimated as an average of three specimens under consideration. The total charge passed can be considered a qualitative measure of a cementitious system's resistance against chloride transport (ASTM C1202).

Rapid Chloride Migration Test

The rapid chloride migration test (RCMT) was conducted as per nord test (NT) Build 492 (1999). The specimen preparation for this method was similar to that of RCPT. Three concrete specimens of 50-mm thickness and 100-mm diameter were obtained from large cylindrical specimens. The initial current obtained when the specimen was subjected to a potential of 30 V was used to determine the duration and final voltage to be applied based on the guidelines provided by NT Build 492 (1999). The non-steady-state migration coefficient indicates the rate at which chloride ions ingress into a cementitious system.

Bulk Diffusion Test

The bulk diffusion test was conducted as per ASTM C1556 (ASTM 2016). Three concrete specimens with 100-mm diameter and 75-mm thickness were obtained from three concrete cylinders after 28 days of curing. After preparation, the specimens were exposed to a concentrated NaCl solution as per ASTM C1556 for 35 days. The powdered samples were collected from various depths, following the guidelines specified in the code. The total chloride and free chloride content were determined using silver nitrate titration as specified in ASTM C1152-22 (ASTM 2012) and ASTM C1218 (ASTM 2015), respectively, using a Metrohm eco titrator (Switzerland).

Results and Discussion

Compressive Strength

Compressive strengths of various binders are shown in Fig. 2. The mix was designed so that the binders under consideration could achieve concrete of M30 grade after 28 days of curing. The rapid hardening expansive and nonexpansive CSAB-based concretes achieved compressive strengths of 29.3 and 30.8 MPa, respectively, in 3 days, which was higher than the 7-day strength (28.9 MPa) achieved by PC concrete. The rate of strength gain of the CSAB cement concrete was observed to be faster than PC concrete, although both CSAB cement and PC concretes achieved almost similar strengths after 28 days of curing. The primary reason for the higher early strength of the CSAB systems could be attributed to the faster rate of hydration of CSAB-based binder systems compared with PC (Shenbagam and Chaunsali 2022).

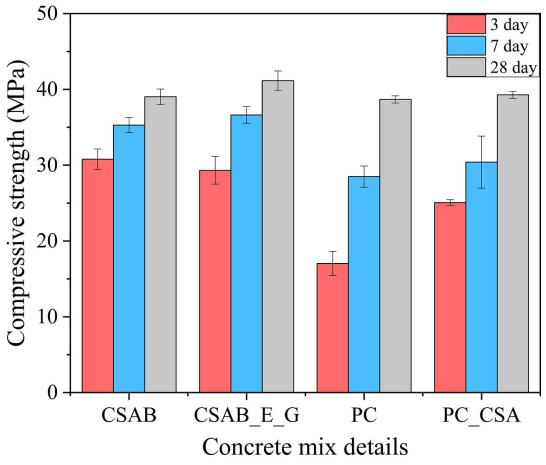

Fig. 2. Compressive strength of concretes having different binders at 3, 7, and 28 days.

The results from this study indicate that the effect of gypsum on the compressive strength of CSAB concrete systems at different ages is limited. The strengths achieved by both CSAB and CSAB_E_G (with added gypsum) were observed to be similar at all ages (3, 7, and 28 days) under consideration. A similar trend was reported in paste and mortar-based studies (Shenbagam and Chaunsali 2022). However, the gypsum addition is reported to promote the precipitation of additional ettringite, which is the primary strength-giving phase in CSAB system (Trauchessec et al. 2015; Winnefeld and Barlag 2009). Addition of CSA admixture improved the hardening of PC concrete. The PC_CSA concrete formulated by adding 10% CSA admixture to PC exhibited improved early-age strength compared with PC. PC_CSA showed a 3-day strength of about 21 MPa (23% higher than PC). Gastaldi et al. (2011) reported that the rapid reaction of ye'elimite present in CSA cement with calcium sulfate in the presence of lime resulted in ettringite formation. The rapid ettringite formation might have contributed to the higher strength gain of PC_CSA mixes during the early ages.

Microstructural Characterization

Phase assemblage of hydrated pastes was determined after 28 days of curing. To examine the influence of chloride ingress on the phase assemblage of the CSAB system, the paste samples were immersed in a 3M NaCl solution for 35 days. Fig. 3 shows the XRD pattern indicating the changes in the phase assemblage of the CSAB and CSAB_E_G systems due to the ingress of chloride ions. The primary hydration product in the CSAB system was found to be ettringite.

The commercial CSAB cement used in this study had a calcium sulfate to ye'elimite molar ratio of about 1.88. The chemical binding capacity of such a system was quite limited, as indicated by a small amount of Friedel's salt that was detected in the system (Fig. 3). The reduced binding capability could be attributed to the lack of monosulfate phase in the system. Unreacted ye'elimite and anhydrite were detected in the CSAB system, which was not exposed to the NaCl solution, possibly due to the lack of available water in the system. The findings of Bernardo et al. (2006) indicated that the water requirement for complete hydration of the CSAB system is higher than PC, indicating the water-cement ratio of 0.5 may be insufficient to cause complete hydration. Furthermore, the amount of ettringite was observed to increase along with a decrease in the amount of ye'elimite and anhydrite in the CSAB system when exposed to NaCl solution, indicating further continuation of hydration in the system.

The CSAB_E_G system, similar to the CSAB system, had ettringite as the main hydrated phase. Contradictory to the CSAB system, the CSAB_E_G system was devoid of ye'elimite due to the blending of gypsum. The addition of gypsum contributed to the formation of ettringite. The chemical binding capacity of CSAB_E_G was further reduced due to the absence of monosulfate, which is evident from the absence of Friedel's salt in paste samples after exposure to a concentrated chloride solution after 35 days.

Fig. 4 shows differential thermogravimetric analysis of the CSAB and CSAB_E_G samples before and after exposure to NaCl solution. The hydrated CSAB and CSAB_E_G binder had predominantly ettringite along with aluminum hydroxide. The CSAB sample had a slight increment in the ettringite peak due to further hydration of ye'elimite. This observation is in line with what was observed

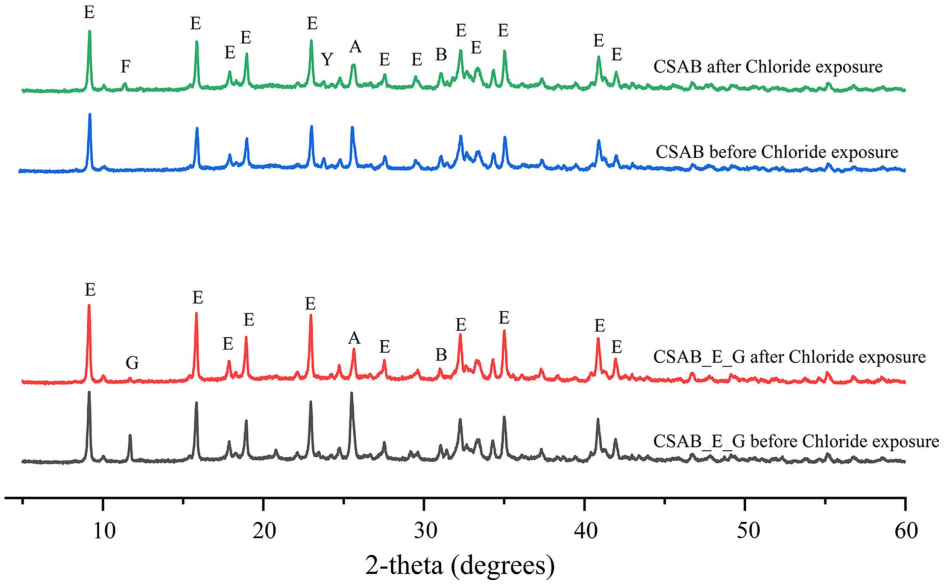

Fig. 3. XRD patterns of the 28-day cured CSAB and CSAB_ E_G cement paste before and after exposure to 3M NaCl solution for 35 days. E: ettringite, A: anhydrite, F: Friedel's salt, Y: ye'elimite, B: belite, and G: gypsum.

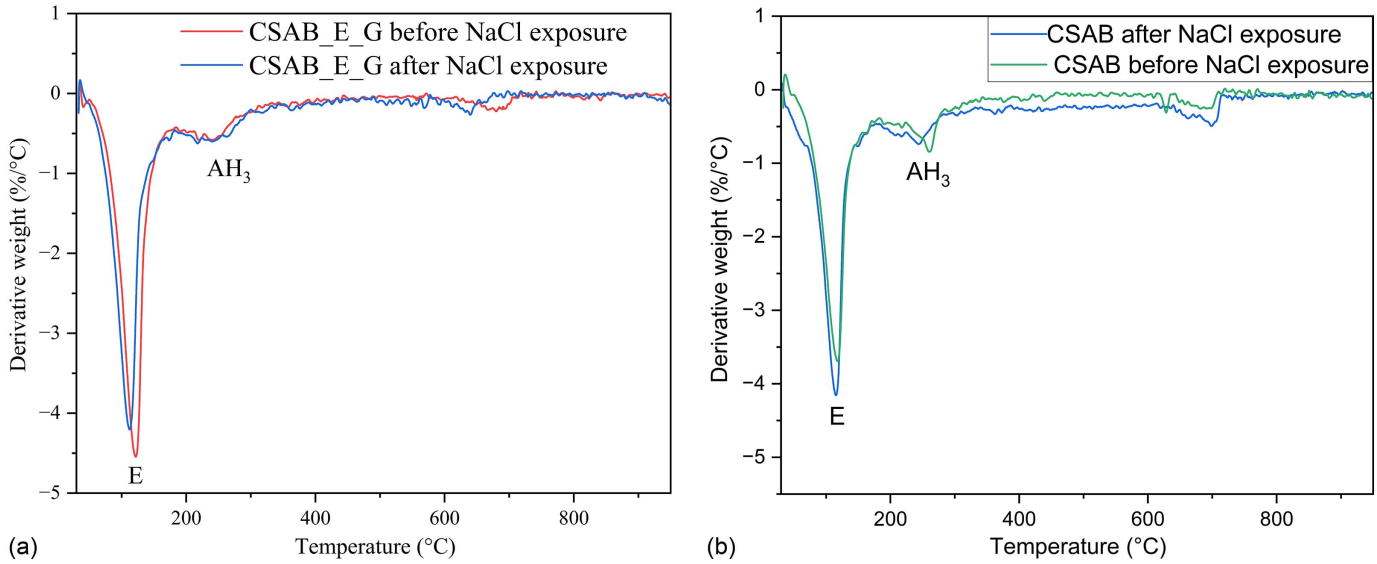

Fig. 4. DTG curves of the 28-day cured cement pastes before and after exposure to 3M NaCl solution for 35 days: (a) CSAB_E_G (blended with gypsum); and (b) CSAB. E: ettringite, and AH_3: aluminum hydroxide.

in the XRD tests. Furthermore, the differential thermogravimetric analysis was not able to capture the presence of Friedel's salt because the amount formed may be quite limited.

Moreover, ettringite and aluminum hydroxide (Fig. 4) present in the CSAB_E_G binder were observed to be stable before and after the exposure to NaCl solution (based on both XRD and TGA). This further indicates that both ettringite and aluminum hydroxide phases do not interact with chloride as reported in previous studies (Jiang et al. 2019; Paul et al. 2015). The slight reduction of the calcium sulfate phase after immersion of the CSAB_E_G specimens in the chloride solution for 35 days could be due to its leaching. This decrease in calcium sulfate is reflected in the XRD pattern, as well as in the differential thermogravimetric (DTG) curve a slight reduction in the main peak after exposure to NaCl. The presence of belite was detected in CSAB and CSAB_E_G systems in both exposed and unexposed samples. The belite was observed to be unreacted in both cases. Further studies are required to understand the influence of belite hydration on chloride transport in the CSAB systems.

To understand the pore structural characteristics of these binder systems, the paste samples prepared with 0.5 w/b ratios were subjected to MIP study; the results are shown in Fig. 5. This section

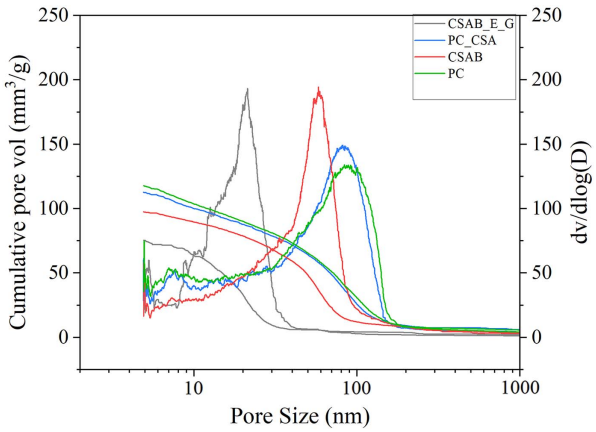

Fig. 5. Cumulative pore size distributions of various binder systems.

provides an in-depth analysis of the pore structure of various binders under consideration with the help of mercury intrusion porosimetry. The CSAB-based systems were observed to have a lower critical pore size and total pore volume when compared with PC-based systems. The critical pore size and total pore volume observed in the nonexpansive CSAB system were higher than those observed in the expansive CSAB system. However, the critical pore size of the nonexpansive CSAB system was lower than that of the PC and PC_CSA, indicating better pore refinement of the CSAB system compared with the PC system.

The CSAB_E_G produced by admixing gypsum has the lowest critical pore size and total pore volume. The critical pore size of CSAB_E_G system was around 21 nm, and 58 nm for the CSAB system. Similarly, the total pore volume in the CSAB_E_G system was 75.5 mm^3/g, whereas for the CSAB system, it was 97.7 mm^3/g. The total pore volume in the expansive CSAB_E_G system was 22% lower when compared with the CSAB system. It was observed that the expansive CSAB_E_G system did not exhibit any microcracking based on the MIP results. The precipitation of ettringite in the pores due to additional gypsum during the hydration was a major contributor to the pore densification in the expansive CSAB cementitious system.

Furthermore, blending of CSA admixture onto PC refined its pore structure. The critical pore size and the total pore volume of the PC_CSA system were lower than those of PC system. The critical pore size of PC_CSA (81.2 nm) was around 9.6% lower than PC (89.8 nm), indicating a decline in the interconnectivity of pores. The pore refinement of PC upon CSA addition was primarily due to the ettringite formation (Trauchessec et al. 2015).

Durability Properties

Sorptivity and Water-Accessible Porosity

Sorptivity and water-accessible porosity results of different mixtures are shown in Fig. 6. Concrete with a denser pore structure had lower pore interconnectivity, resulting in reduced moisture transport. The CSAB concrete system had better pore refinement (reduced sorptivity index) than the PC-based concrete system. The pore refinement due to ettringite formation in the CSAB system reduced the

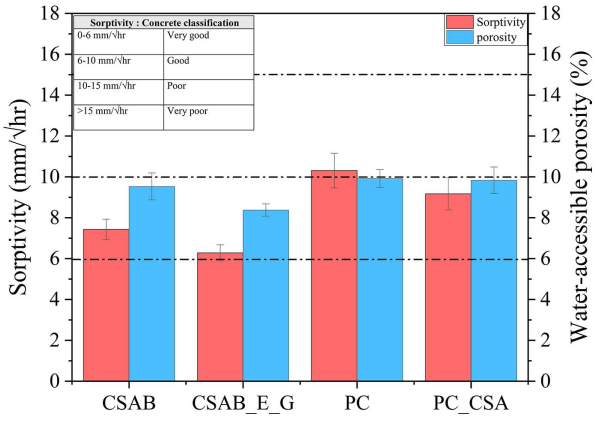

Fig. 6. Sorptivity and water-accessible porosity of concretes having different binders.

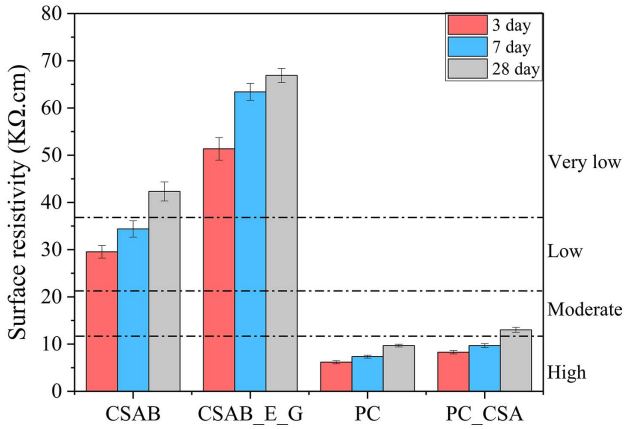

Fig. 7. Surface resistivity of concretes having different binders using Wenner probe.

interconnectivity of pores. Furthermore, based on the results, the expansive CSAB cement concrete (CSAB_E_G) had the lowest sorptivity value, followed by CSAB, PC_CSA, and PC. Based on the classification provided by Alexander et al. (2010), both expansive and nonexpansive CSAB cement concretes could be classified as having a good resistance against water absorption based on the water sorptivity index. In contrast, PC concrete was classified as having poor quality. However, the use of a CSA admixture in PC improved its resistance against moisture transport.

Water-accessible porosity was determined from the same specimen after conducting the sorptivity test. The water-accessible porosity indicates a part of air voids and saturated porosity of the cement paste of concrete system (Bu et al. 2014). The water-accessible porosity (Fig. 6) was observed to be the least for the expansive CSAB system. However, the variation between the porosity values of various binders was minimal because all the concrete mixtures under consideration conformed to a similar strength grade.

Evolution of Surface Resistivity

Electrical resistivity of concrete system is used as a durability indicator, providing an understanding of the interconnectivity of pores (Bediwy and Bassuoni 2018). Resistivity refers to a system's resistance against ionic transport. The resistivity of concrete affects the initiation and propagation of steel corrosion in a reinforced concrete system (Feliu et al. 1996; González et al. 2004; Hope et al. 1985; Liu and Weyers 1998; Morris et al. 2004). A strong correlation between chloride ingress and the resistivity of concrete systems has been shown by several studies (Dhandapani and Santhanam 2022; Ghosh and Tran 2015; Lim et al. 2011; Ramezanianpour et al. 2011; Santhanam 2017; Tanesi and Ardani 2012). A concrete system with higher resistivity will limit the mobility of ions, consequently reducing the corrosion rate and improving its durability and service life. The investigations conducted by Polder (2009) showed a linear relationship between electrical resistivity and the probability of corrosion. The surface resistivity can be directly correlated with the bulk resistivity of concrete and can be used as an indirect measure of concrete's transport characteristics (Ghosh and Tran 2015).

The surface resistivity values of concrete mixtures at various ages are shown in Fig. 7. In all the binder systems, the surface resistivity values increased with age. The surface resistivity of expansive and nonexpansive CSAB systems developed rapidly compared with the PC concrete system. The surface resistivity of CSAB_E_G and CSAB systems at 3 days was several times higher than PC system. The hydration of CSAB-based system is very rapid, leading to pore refinement (or densification) at an early age compared with PC

Table 5. Pore solution conductivity of binders at 3, 7, and 28 days

	Pore solution conductivity (S/m)		
Binder	3 days	7 days	28 days
CSAB	2.79	2.65	2.53
CSAB_E_G	2.18	2.12	2.09
PC	4.48	4.86	5.28
PC_CSA	4.28	4.71	5.44

(Shenbagam and Chaunsali 2022). The rapid development in surface resistivity correlated well with strength development. With regard to surface resistivity, the binder systems used in this study could be ranked in the following order: CSAB_E_G > CSAB > PC_CSA > PC.

The surface resistivity of the expansive CSAB system was observed to be higher than nonexpansive CSAB system. Higher resistivity could be attributed to the pore refinement due to the precipitation of ettringite in the presence of admixed gypsum, along with lower pore solution conductivity (Table 5). The addition of CSA admixture to PC increased the surface resistivity of the system. The PC_CSA system was observed to have higher surface resistivity from an early age of hydration and followed a similar trend until 28 days of curing. The enhanced resistivity observed in the PC_CSA system, compared with conventional PC, can be attributed to the refined pore structure of the system, as indicated by similar pore solution conductivity to the PC binder system.

The surface resistivity can be used as an indicator for the resistance of a concrete system against chloride ion ingress. The FM-5-578 test method (FDOT 2004) classifies the quality of various concrete systems against chloride ion permeability based on surface resistivity. The FM-5-578 classification of different binder systems is depicted in Fig. 7. The classification based on surface resistivity shows that the expansive CSAB system (CSAB_E_G) had a very low chloride ingress from a very early age of curing. The nonexpansive CSAB system achieved a very low risk of chloride ingress within 7 days of curing. The PC_CSA concrete system can be classified as having a moderate chloride ion permeability, whereas PC concrete had a high chloride ion permeability. This classification, based on surface resistivity values, indicates that both expansive and nonexpansive CSAB systems had excellent resistance against chloride ingress. However, the influence of pore solution conductivity on surface resistivity cannot be neglected. To further understand the role of pore refinement on these systems, a formation factor approach was adopted.

The formation factor is a material property well-linked with the transport properties of a cementitious system (Spragg et al. 2016; Weiss et al. 2018). The formation factor is inversely correlated to the porosity and pore connectivity factor. The resistivity of a cementitious system can be considered a good indicator of the pore refinement of different binder systems. However, the results could be influenced by the pore solution conductivity of the system. The hydrated phase assemblage of CSAB systems differs from that of PC, resulting in potentially significant distinctions in the pore solution conductivity between these binders.

The formation factor is a material property of a system, which can be correlated to its transport properties. Archie's law establishes a relationship among the conductivity of the system, pore solution conductivity, and pore structure factor (Archie 1942). Furthermore, the Nernst-Einstein relationship [Eq. (1)], can be used to interpret the relationship between the formation factor and the effective diffusion coefficient. This integration holds significant potential for enhancing the understanding of the interplay between electrical properties and transport phenomena within porous media

$$F = \frac{1}{\varphi^{m}} = \frac{\sigma_0}{\sigma_{eff}} = \frac{D_0}{D} \tag{1}$$

where F = formation factor; φ = capillary porosity; m = pore connectivity factor; D_0 = ionic diffusion coefficient; D = bulk diffusion coefficient; σ_{eff} = bulk conductivity; and σ_0 = pore solution conductivity.

The formation factor based on Eq. (1) can be interpreted as the ratio between bulk resistivity and the resistivity of the pore solution. The conductivity of pore solution extracted from hydrated pastes at various curing ages is provided in Table 5. The bulk resistivity of the concrete system can be directly correlated with the surface resistivity data obtained from the Wenner probe with the help of a correction factor (Spragg et al. 2013). The correction factors are applicable for conditions of $d/a \leq 6$ or $L/a \geq 6$. Based on the dimensions of the specimen used, the correction factor was determined to be in the range of 1.86–1.88 (sight variation in diameter of the cylindrical specimen), considering the dimension of the concrete cylinder used. The bulk resistivity is calculated based on Eq. (2) (Baten and Manzur 2022)

$$\rho = R \times k \tag{2}$$

where ρ = bulk resistivity; R = surface resistivity obtained through the Wenner probe; and k = 1/1.88 to 1/1.86 based on the correction factor obtained.

The bulk resistivity, as previously mentioned, was utilized along with the pore solution conductivity values to determine the formation factor. The change in formation factor of various binders with curing age, along with the classification of the concrete system (based on formation factor) against chloride ingress as per AASHTO PP-84 (AASHTO 2017)], is given in Fig. 8.

The evolution of formation factor with curing age follows a similar trend as observed in surface resistivity. The CSAB systems have higher formation factor values when compared with PC-based systems. The improvement in the formation factor observed in CSAB systems after 7 days of curing is relatively minimal compared with PC-based systems. This observation aligns with the hydration characteristics of these cementitious systems.

The pore solution conductivity of the CSAB systems is lower than that of the PC-based systems, indicating a higher pore solution resistivity when compared with PC-based systems. The pore solution conductivity of the CSAB systems seems to have significantly contributed to increasing the surface resistivity of these systems. The CSAB systems based on formation factor are classified as having only moderate resistance to chloride ingress even though these

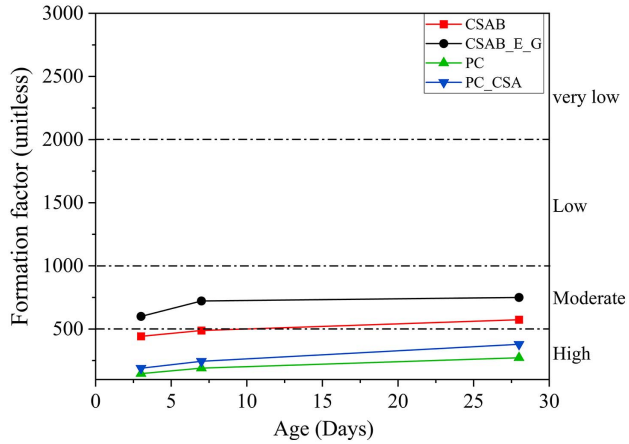

Fig. 8. Variation of formation factor with curing age. The k values under consideration are CSAB = 0.536, CSAB_E_G = 0.538, PC = 0.533, and PC_CSA = 0.536.

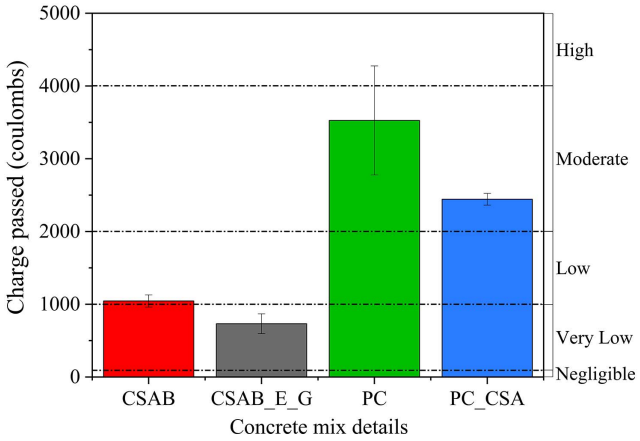

Fig. 9. Charge passed through different binders based on RCPT.

systems have a very high surface resistivity. Given that the transport of chloride ions is significantly dependent on the pore structure of the cementitious system, formation factor–based classification of CSAB systems could be a better indicator of its real-world performance.

Resistance against Chloride Transport

The amount of charge passed in the RCPT provides a measure of the resistance of a concrete system against chloride ingress. The RCPT results of the various concrete mixtures under consideration are shown in Fig. 9. The results based on the total amount of charge passed indicate that the performance of both expansive and nonexpansive CSAB concrete systems was better than PC concrete. The qualitative classification based on ASTM C1202 categorizes the expansive CSAB system (CSAB_E_G) into the very low charge passed category. The expansive CSAB system had very limited to zero chemical binding capacity due to the absence of an AFm phase. The additional gypsum favored ettringite formation, resulting in the absence of monosulfate.

Characterization studies indicated that the ettringite phase had negligible chloride binding capacity. Although the binding capacity of expansive CSAB cement was limited, the precipitation of ettringite led to the refinement of the pore size distribution. The denser microstructure, along with lower pore solution conductivity, was the primary cause behind the performance of expansive CSAB system.

Furthermore, the nonexpansive CSAB system was characterized by a low amount of charge passed. The nonexpansive CSAB system's ability to bind chlorides was lower than the PC system (Alapati et al. 2022). However, a highly refined pore structure in the nonexpansive CSAB system enabled it to have a lower amount of charge passed than PC concrete.

Furthermore, the addition of a CSA admixture to PC concrete led to pore structure refinement of the system. Although both PC and PC_CSA systems can be classified as having a moderate amount of charge passed, the addition of CSA admixture to PC considerably reduced the total charge passed in PC_CSA cement concrete when compared with PC. RCMT was also performed to assess the chloride resistance of various binders in the form of non-steady-state migration coefficient. The migration coefficient, i.e., the rate of chloride transport under an applied potential, gives a quantitative measure of chloride resistance of concrete system under consideration.

The non-steady-state migration coefficients obtained for various binder systems after 28 days of curing are provided in Fig. 10. The results obtained followed a similar trend to the observed RCPT results. The non-steady-state migration coefficient was observed to be lowest for the expansive CSAB (CSAB_E_G) concrete system, indicating the difficulty of chloride ions to ingress through a highly dense pore structure of the expansive CSAB system. The expansive CSAB (CSAB_E_G) and nonexpansive CSAB concrete systems had about 63% and 44% lower chloride migration coefficients, respectively, compared with PC concrete. Furthermore, adding the CSA admixture to PC reduced the rate of chloride ingress by 15%. The standard deviation of the RCPT results of the PC system obtained was higher than the recommended range as per ASTM C1202. However, the minimum value for PC system was higher than the RCPT values for all the binders under consideration.

The classification of different concretes under consideration based on RILEM TC 230 (Bjegović et al. 2016) is listed in Fig. 10. The expansive (CSAB_E_G) system was classified as having good resistance against chloride ingress. In contrast, the nonexpansive CSAB system was classified as having normal resistance against chloride ion ingress. The chloride ingress observed in the CSAB-based binder system was lower compared with PC, which was classified as having poor resistance against chloride penetration. Although adding CSA admixture to PC improved the system's resistance against chloride, the PC_CSA system was classified as having poor resistance against chloride ingress. The lower migration coefficient observed in CSAB systems could be exclusively attributed to the pore refinement of CSAB cement concrete.

The formation factor–based approach categorizes the CSAB system as exhibiting only moderate resistance to chloride ingress. The reduced pore solution conductivity could have played a role in influencing the outcomes of the migration-based tests. Both RCPT and RCMT are accelerated migration-based tests conducted by applying a certain voltage. To further understand the nature of these binders in a chloride-rich environment, long-term bulk diffusion-based tests were conducted as per ASTM C1556. The bulk diffusion–based test depends on the diffusion of chlorides onto the concrete systems. The performance of these concrete systems will depend on the pore refinement and binding capability of these systems. The apparent diffusion coefficient of the binders under consideration is given in Fig. 11.

The diffusion coefficient values of all the systems were observed to be in a similar range. The PC_CSA system outperformed the other binders by a narrow margin. The results obtained from the accelerated migration-based test do not correlate with the long-term bulk diffusion tests. The CSAB system was observed to outperform PC-based systems based on accelerated test results. The results from the accelerated migration techniques suggest that in CSAB cementitious systems, the movement of ions is primarily influenced by the process of pore refinement (Ioannou et al. 2015). Nevertheless, long-term studies based on ASTM C1556 indicate that chloride binding significantly affects the chloride resistance of a concrete system.

Although the expansive CSAB_E_G system had better pore refinement than nonexpansive CSAB system, the absence of chemical binding of chlorides might have been the reason for similar performance of these systems. Although PC concrete exhibits a relatively coarser pore structure compared with CSAB systems, it possesses superior binding capabilities, thereby leading to comparable performance to CSAB systems. The total, free, and bound chloride data obtained from powdered samples obtained from the concrete systems under consideration are given in Fig. 12.

The total and free chlorides were determined based on acid and water-soluble titration on the profiled concrete powder as per ASTM C1152 and ASTM C1218, respectively. Moreover, the bound chloride was determined as the difference between total and free chloride profiles. The binding capacity of the PC system was observed to be the highest, closely followed by the PC_CSA system. Nevertheless, results from long-term bulk diffusion tests indicate that caution should be exercised when selecting test methods for determining the chloride resistance of CSAB-based systems because migration-based

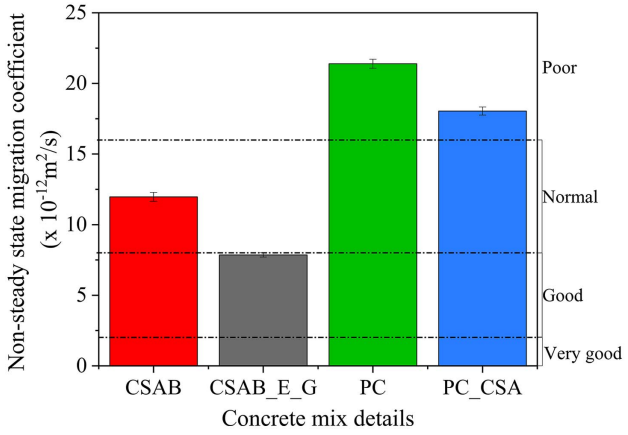

Fig. 10. Nonsteady chloride migration coefficients of concretes having different binders.

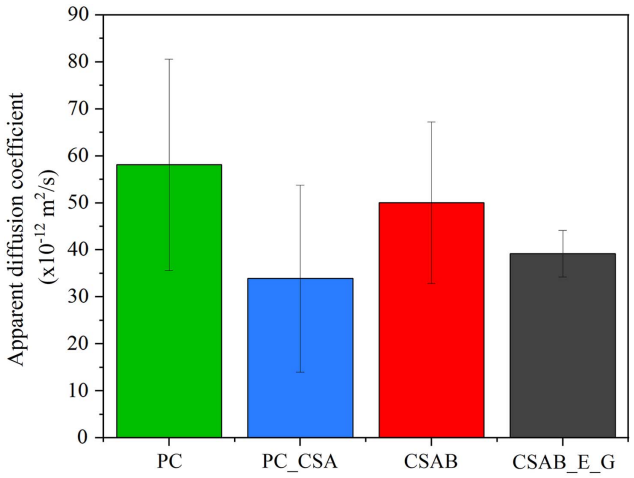

Fig. 11. Apparent diffusion coefficient of various binder systems based on ASTM C1556.

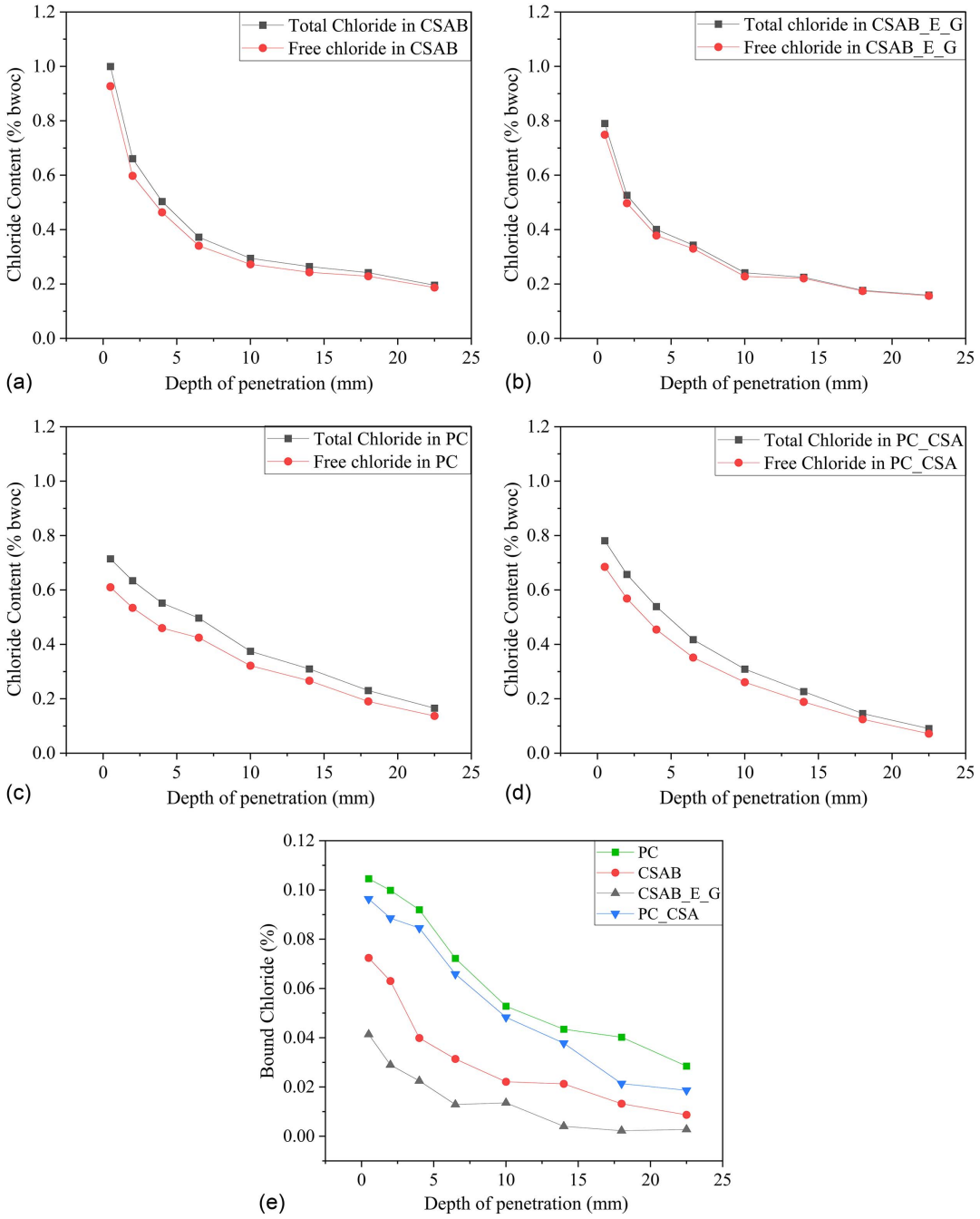

Fig. 12. Chloride data of different concrete systems obtained from powder collected at different depths: (a) total and free chloride data of CSAB; (b) total and free chloride data of CSAB_E_G; (c) total and free chloride data of PC; (d) total and free chloride data of PC_CSA; and (e) bound chloride of different concrete systems under consideration.

accelerated test methods may not be suitable for CSAB-based concrete systems.

The chloride transport–based assessment on these binder systems indicated that accelerated migration-based test results did not correlate well with the long-term test results. The performance of all the binders was observed to be similar in bulk diffusion-based tests. The pore structure might be an influencing factor in accelerated migration–based test. Furthermore, the pore solution conductivity might have also influenced these results. Surface resistivity measurements of the CSAB system demonstrated superior performance in comparison with PC-based systems. However, the formation factor–based approach, which mitigates the influence of pore solution conductivity, offers a more accurate indication of the pore structure refinement within these binder systems.

Although the formation factor trend aligned with the observations from the surface resistivity tests, the difference among the binders was less pronounced. The long-term bulk diffusion–based test results are more representative of field condition. The results indicate that the CSAB-based binder used in this study had similar performance to PC-based systems in a chloride-rich environment. The PC_CSA-based system had slightly better performance than the other systems under consideration.

Furthermore, the total, free, and bound chlorides in the cementitious systems were also determined. The observations indicate that the binding capability of the CSAB system was negligible when

compared with PC-based systems. The CSAB_E_G system had the least binding capability, followed by the nonexpansive CSAB system. The PC system had the highest chloride binding capacity and the blending of CSA admixture with PC decreased its binding capacity marginally.

In this study, the performance of different concretes against chloride ingress was assessed using accelerated migration–based tests and long-term immersion-based tests. However, the corrosion of reinforcing steel in CSAB cement–based concrete systems needs a detailed investigation. The capability of CSAB system in passivating the steel reinforcement due to the low pH of the system requires further study. The resistivity of the CSAB system was observed to be higher than PC, and the influence of this resistivity on corrosion propagation needs to be addressed because it can be a contributing factor toward the system's service life.

Conclusions

Based on the current study, the following conclusions can be drawn:

- Both expansive and nonexpansive CSAB systems exhibited higher surface resistivity than PC-based systems of similar strength. However, the pore solution conductivity of CSAB system was much lower than PC based system, making the formation factor a realistic representation of resistance to chloride ingress.
- Compared with the PC-based system, both expansive and nonexpansive CSAB systems performed better against chloride ingress based on RCPT and RCMT tests. The chloride resistance of the binders followed the trend of CSAB_E_G > CSAB > PC_CSA > PC. However, the long-term bulk diffusion test results indicated similar chloride resistance of these systems.
- The pore refinement of the expansive CSAB_E_G system was found to be superior to all the other binders under consideration. However, the capacity of the system to chemically bind chlorides was nonexistent, as evident from the lack of Friedel's salt formation based on XRD analysis. The slight amount of bound chloride observed may be due to the physical binding of these chlorides by the hydrated phases.
- The performance of PC systems blended with a CSA admixture was slightly better than the other binders under consideration due to the improvement in pore refinement while retaining similar binding capacity of the blended PC_CSA system.

Data Availability Statement

Some or all data, models, or code that support the findings of this study are available from the corresponding author upon reasonable request.

Acknowledgments

The authors gratefully acknowledge the support from the Department of Civil engineering at IIT Madras toward providing all the facilities and equipment required for the testing. The first author would like to acknowledge the All-India Council of Technical Education (AICTE) for the Ph.D. scholarship. The last author is grateful for the financial support from the New Faculty Seed Grant by Industrial Consultancy and Sponsored Research (ICSR) Centre at IIT Madras. The Centre of Excellence grant on Technologies for Low Carbon and Lean Construction (TLC2) from IIT Madras is also gratefully acknowledged.

References

AASHTO. 2017. *Standard practice for developing performance engineered concrete pavement mixtures*. AASHTO PP 84. Washington, DC: AASHTO.

Alapati, P., M. K. Moradllo, N. Berke, M. T. Ley, and K. E. Kurtis. 2022. "Designing corrosion resistant systems with alternative cementitious materials." *Cement* 8 (Jun): 100029. https://doi.org/10.1016/j.cement.2022.100029.

Alexander, M., Y. Ballim, and J. M. Mackechnie. 2018. "Durability index testing procedure manual." *Res. Monogr.* 2018 (Feb): 29.

Alexander, M. G., M. Santhanam, and Y. Ballim. 2010. "Durability design and specification for concrete structures—The way forward." *Int. J. Adv. Eng. Sci. Appl. Math.* 2 (3): 95–105. https://doi.org/10.1007/s12572-011-0027-x.

Archie, G. E. 1942. "The electrical resistivity log as an aid in determining some reservoir characteristics." *Trans. AIME* 146 (1): 54–62.

ASTM. 2012. *Standard test method for acid-soluble chloride in mortar and concrete*. ASTM C1152-22. West Conshohocken, PA: ASTM.

ASTM. 2015. *Standard test method for water-soluble chloride in mortar and concrete*. ASTM C1218. West Conshohocken, PA: ASTM.

ASTM. 2016. *Determining the apparent chloride diffusion coefficient of cementitious mixtures by bulk diffusion*. ASTM C1556-11a. West Conshohocken, PA: ASTM.

ASTM. 2019. *Standard test method for electrical indication of concrete's ability to resist chloride ion penetration*. ASTM C1202. West Conshohocken, PA: ASTM.

ASTM. 2020. *Standard practice for mechanical mixing of hydraulic cement pastes and mortars of plastic consistency*. ASTM C305-20. West Conshohocken, PA: ASTM.

Baten, B., and T. Manzur. 2022. "Formation factor concept for nondestructive evaluation of concrete's chloride diffusion coefficients." *Cem. Concr. Compos.* 128 (May): 104440. https://doi.org/10.1016/j.cemconcomp.2022.104440.

Bediwy, A., and M. T. Bassuoni. 2018. "Resistivity, penetrability and porosity of concrete: A tripartite relationship." *J. Test. Eval.* 46 (2): 20160374. https://doi.org/10.1520/JTE20160374.

Bernardo, G., A. Telesca, and G. L. Valenti. 2006. "A porosimetric study of calcium sulfoaluminate cement pastes cured at early ages." *Cem. Concr. Res.* 36 (6): 1042–1047. https://doi.org/10.1016/j.cemconres.2006.02.014.

BIS (Bureau of Indian Standards). 2000. *Plain and reinforced concrete—Code of practice*. IS 456. New Delhi, India: BIS.

BIS (Bureau of Indian Standards). 2015. *Ordinary portland cement–specification*. IS 269:2015. New Delhi, India: BIS.

BIS (Bureau of Indian Standards). 2016. *Coarse and fine aggregate for concrete–specification*. IS:383 (2016). New Delhi, India: BIS.

BIS (Bureau of Indian Standards). 2018. *Method of tests for strength of concrete*. IS 516—Part I. New Delhi, India: BIS.

Bizzozero, J., C. Gosselin, and K. L. Scrivener. 2014. "Expansion mechanisms in calcium aluminate and sulfoaluminate systems with calcium sulfate." *Cem. Concr. Res.* 56 (Feb): 190–202. https://doi.org/10.1016/j.cemconres.2013.11.011.

Bjegović, D., M. Serdar, I. S. Oslakovi, F. Jacobs, H. Beushausen, C. Andrade, A. V. Monteiro, P. Paulini, and S. Nanukuttan. 2016. "Test methods for concrete durability indicators." In *Performance-based specifications and control of concrete durability: State-of-the-art report RILEM TC 230-PSC*, 51–105. Cité Descartes, France: RILEM.

Bu, Y., R. Spragg, and W. J. Weiss. 2014. "Advances in civil engineering materials comparison of the pore volume in concrete as determined using ASTM C642 and vacuum saturation." 3 (1): 308–315. https://doi.org/10.1520/ACEM20130090.

Chaunsali, P., and K. Vaishnav. 2020. "Calcium-sulfoaluminate-belite cements: Opportunities and challenges." *Indian Concr. J.* 94 (Jun): 18–25.

Chen, I. A., C. W. Hargis, and M. C. G. G. Juenger. 2012. "Understanding expansion in calcium sulfoaluminate-belite cements." *Cem. Concr. Res.* 42 (1): 51–60. https://doi.org/10.1016/j.cemconres.2011.07.010.

Dhandapani, Y., and M. Santhanam. 2017. "Assessment of pore structure evolution in the limestone calcined clay cementitious system and its

implications for performance." *Cem. Concr. Compos.* 84 (Jun): 36–47. https://doi.org/10.1016/j.cemconcomp.2017.08.012.
Dhandapani, Y., and M. Santhanam. 2022. "On the correlations between different chloride transport parameters and their role in service life estimation." *Sustainable Resilient Infrastruct.* 8 (2): 240–255. https://doi.org/10.1080/23789689.2022.2097771.
FDOT (Florida Department of Transportation). 2004. *Florida method of test for concrete resistivity as an electrical indicator of its permeability.* FM 5-578. Tallahassee, FL: FDOT.
Feliu, S., J. A. Gonzalez, and C. Andrade. 1996. "Electrochemical methods for on-site determinations of corrosion rates of rebars." In *Techniques to assess the corrosion activity of steel reinforced concrete structures*, edited by N. S. Berke, E. Escalante, C. K. Nmai, and D. Whiting. West Conshohocken, PA: ASTM.
Florea, M. V. A., and H. J. H. Brouwers. 2012. "Cement and concrete research chloride binding related to hydration products Part I: Ordinary portland cement." *Cem. Concr. Res.* 42 (2): 282–290.
Gartner, E. 2004. "Industrially interesting approaches to 'low-CO_2' cements." *Cem. Concr. Res.* 34 (9): 1489–1498.
Gastaldi, D., F. Canonico, L. Capelli, M. Bianchi, M. Pace, A. Telesca, and G. Valenti. 2011. "Hydraulic behaviour of calcium sulfoaluminate cement alone and in mixture with portland cement." In *Proc., 13th Int. Congress on the Chemistry of Cement*, 1–7. Amsterdam, Netherlands: Elsevier.
Ghosh, P., and Q. Tran. 2015. "Influence of parameters on surface resistivity of concrete." *Cem. Concr. Compos.* 62 (Sep): 134–145. https://doi.org/10.1016/j.cemconcomp.2015.06.003.
Glasser, F. P., and L. Zhang. 2001. "High-performance cement matrices based on calcium sulfoaluminate-belite compositions." *Cem. Concr. Res.* 31 (12): 1881–1886. https://doi.org/10.1016/S0008-8846(01)00649-4.
González, J. A., J. M. Miranda, and S. Feliu. 2004. "Considerations on reproducibility of potential and corrosion rate measurements in reinforced concrete." *Corros. Sci.* 46 (10): 2467–2485. https://doi.org/10.1016/j.corsci.2004.02.003.
Hanein, T., J. Galvez-Martos, and M. N. Bannerman. 2018. "Carbon footprint of calcium sulfoaluminate clinker production." *J. Cleaner Prod.* 172 (Jan): 2278–2287. https://doi.org/10.1016/j.jclepro.2017.11.183.
Hargis, C. W., C. J. Muller, B. Lothenbach, and F. Winnefeld. 2018. "Further insights into calcium sulfoaluminate cement expansion." *Adv. Cem. Res.* 31 (4): 160–177. https://doi.org/10.1680/jadcr.18.00124.
Hope, B. B., A. K. Ip, and D. G. Manning. 1985. "Corrosion and electrical impedance in concrete." *Cem. Concr. Res.* 15 (3): 525–534. https://doi.org/10.1016/0008-8846(85)90127-9.
Ioannou, S., K. Paine, L. Reig, and K. Quillin. 2015. "Performance characteristics of concrete based on a ternary calcium sulfoaluminate-anhydrite-fly ash cement." *Cem. Concr. Compos.* 55 (Jan): 196–204. https://doi.org/10.1016/j.cemconcomp.2014.08.009.
Jen, G., N. Stompinis, and R. Jones. 2017. "Chloride ingress in a belite-calcium sulfoaluminate cement matrix." *Cem. Concr. Res.* 98 (Aug): 130–135. https://doi.org/10.1016/j.cemconres.2017.02.013.
Jiang, X., Z. Zhong, and W. Liu. 2019. "Influence of mineral admixture in CSA cement on chloride binding capacity." In Vol. 283 of *Proc., IOP Conf. Series: Earth and Environmental Science*, 012014. Bristol, UK: IOP.
Juenger, M. C. G., F. Winnefeld, J. L. Provis, and J. H. Ideker. 2011. "Advances in alternative cementitious binders." In *Cement and concrete research*. New York: Elsevier.
Lim, D. T. Y., B. S. Divsholi, D. Xu, and S. Teng. 2011. "Evaluation of high performance concrete using electrical resistivity technique." In *Proc., 36th Conf. on Our World in Concrete and Structures*, 14–16. Singapore: CI-Premier.
Liu, T., and R. W. Weyers. 1998. "Modeling the dynamic corrosion process in chloride." *Cem. Concr. Res.* 28 (3): 365–379. https://doi.org/10.1016/S0008-8846(98)00259-2.
Morris, W., A. Vico, and M. Vázquez. 2004. "Chloride induced corrosion of reinforcing steel evaluated by concrete resistivity measurements." *Electrochim. Acta* 49 (25): 4447–4453. https://doi.org/10.1016/j.electacta.2004.05.001.
NT Build 492. 1999. *Concrete, mortar and cement-based repair materials: Chloride migration coefficient from non-steady-state migration experiments*, 1–8. Espoo, Finland: Nordtest.
Paul, G., E. Boccaleri, L. Buzzi, F. Canonico, and D. Gastaldi. 2015. "Friedel's salt formation in sulfoaluminate cements: A combined XRD and 27Al MAS NMR study." *Cem. Concr. Res.* 67 (Jan): 93–102. https://doi.org/10.1016/j.cemconres.2014.08.004.
Polder, R. B. 2009. "Critical chloride content for reinforced concrete and its relationship to concrete resistivity." *Mater. Corros.* 60 (8): 623–630. https://doi.org/10.1002/maco.200905302.
Ramezanianpour, A. A., A. Pilvar, M. Mahdikhani, and F. Moodi. 2011. "Practical evaluation of relationship between concrete resistivity, water penetration, rapid chloride penetration and compressive strength." *Constr. Build. Mater.* 25 (5): 2472–2479. https://doi.org/10.1016/j.conbuildmat.2010.11.069.
Santhanam, B. S. D. M. 2017. "Performance evaluation of rapid chloride permeability test in concretes with supplementary cementitious materials." *Mater. Struct.* 50 (1): 1–9. https://doi.org/10.1617/s11527-016-0940-3.
Shenbagam, V. K., R. Cepuritis, and P. Chaunsali. 2021. "Influence of exposure conditions on expansion characteristics of lime-rich calcium sulfoaluminate-belite blended cement." *Cem. Concr. Compos.* 118 (Apr): 103932. https://doi.org/10.1016/j.cemconcomp.2021.103932.
Shenbagam, V. K., and P. Chaunsali. 2022. "Influence of calcium hydroxide and calcium sulfate on early-age properties of non-expansive calcium sulfoaluminate belite cement." *Cem. Concr. Compos.* 128 (Apr): 104444. https://doi.org/10.1016/j.cemconcomp.2022.104444.
Spragg, R., Y. Bu, K. Snyder, D. Bentz, and J. Weiss. 2013. *Electrical testing of cement-based materials: Role of testing techniques, sample conditioning, and accelerated curing*. Indianapolis, IN: Indiana Department of Transportation.
Spragg, R., C. Villani, and J. Weiss. 2016. "Electrical properties of cementitious systems: Formation factor determination and the influence of conditioning procedures." *Adv. Civ. Eng. Mater.* 5 (1): 124–148. https://doi.org/10.1520/ACEM20150035.
Tanesi, J., and A. Ardani. 2012. *Surface resistivity test evaluation as an indicator of the chloride permeability of concrete*. Rep. No. FHWA-HRT-13-024. Washington, DC: Federal Highway Administration.
Trauchessec, R., J. M. Mechling, A. Lecomte, A. Roux, and B. Le Rolland. 2015. "Hydration of ordinary Portland cement and calcium sulfoaluminate cement blends." *Cem. Concr. Compos.* 56 (Feb): 106–114. https://doi.org/10.1016/j.cemconcomp.2014.11.005.
Weiss, W. J., R. P. Spragg, O. B. Isgor, M. T. Ley, and T. Van Dam. 2018. *Toward performance specifications for concrete: Linking resistivity, RCPT and diffusion predictions using the formation factor for use in specifications BT–High tech concrete: Where technology and engineering meet*, edited by D. A. Hordijk and M. Luković, 2057–2065. Berlin: Springer.
Winnefeld, F., and S. Barlag. 2009. "Influence of calcium sulfate and calcium hydroxide on the hydration of calcium sulfoaluminate clinker." *ZKG Int.* 62 (12): 42–53.
Zhao, J., G. Cai, D. Gao, and S. Zhao. 2014. "Influences of freeze-thaw cycle and curing time on chloride ion penetration resistance of sulphoaluminate cement concrete." *Constr. Build. Mater.* 53 (Aug): 305–311. https://doi.org/10.1016/j.conbuildmat.2013.11.110.
Zhou, Q., N. B. Milestone, and M. Hayes. 2006. "An alternative to portland cement for waste encapsulation-The calcium sulfoaluminate cement system." *J. Hazards Mater.* 136 (1): 120–129. https://doi.org/10.1016/j.jhazmat.2005.11.038.